A cost-effective combination of Rose Bengal and off-the-shelf cationic polystyrene for the photodynamic inactivation of *Pseudomonas aeruginosa*

Carla Arnau del Valle,[a] *Vanesa Pérez-Laguna*,[b] *Ignacio Muñoz Resta*,[a] *Raquel Gavara*,[a] *Carles Felip-León*,[a] *Juan F. Miravet*,[a] *Antonio Rezusta*,[b,*] *Francisco Galindo* [a,*]

[a] Universitat Jaume I, Departamento de Química Inorgánica y Orgánica, Avda. Sos Baynat s/n, 12071, Castellón, Spain.

[b] Departamento de Microbiología, Hospital Universitario Miguel Servet, IIS Aragón, Zaragoza, Spain.

* Corresponding authors.

E-mail addresses: arezusta@unizar.es (A. Rezusta), francisco.galindo@uji.es (F. Galindo).

KEYWORDS: bactericidal materials, antimicrobial photodynamic inactivation, singlet oxygen, photosensitizers, Rose Bengal

ABSTRACT. Two new photoactive materials have been prepared, characterized and tested against *Pseudomonas aeruginosa* bacteria (planktonic suspension). The synthesis of the polymeric photosensitizers can be made at a multigram scale, in few minutes, starting from inexpensive and readily available materials, such as Rose Bengal (photosensitizer) and ion exchange resins Amberlite® IRA 900 (macroporous) or IRA 400 (gel-type) as cationic polystyrene supports. The most notable feature of these systems is their notable bactericidal activity in the dark (4-5 $\log_{10}$ CFU / mL reduction of the population of *P. aeruginosa*) which becomes enhanced upon irradiation with visible light (to reach a total reduction of 8 $\log_{10}$ CFU / mL for the macroporous polymer at a fluence of 120 J/cm^2 using green light of 515 nm).

1. Introduction

Nosocomial, or hospital-acquired, infections are a rampant problem for national health services, causing yearly hundreds of thousands of deaths worldwide.[1] Signs of alert have been increasing during the last decade and cannot be overlooked. In 2008 Rice coined the acronym ESKAPE to describe the group of bacteria causing the most frequent nosocomial infections (*Enterococcus faecium*, *Staphylococcus aureus*, *Klebsiella pneumoniae*, *Acinetobacter baumannii*, *Pseudomonas aeruginosa* and *Enterobacter species*),[2] and the World Health Organization (WHO) has recently warned about the need for new therapeutic approaches to treat antibiotic-resistant bacteria.[3] Bacteria identified by the WHO as serious threats for the human health in the whole world include 12 species. In this list, *P. aeruginosa* is classified within the most dangerous class "Priority 1: critical". The number of adverse clinical scenarios associated to this pathogen includes not only chronic respiratory infections, sepsis and lung damage in children with cystic fibrosis, but also infections related to surgical wounds / catheters, recurrent pneumonia,

sepsis, urinary tract infections and a long list of other problems in immunocompromised patients. Despite the concentrated efforts of the scientific community to develop alternatives to the existing antibiotics,[4,5] the current realistic therapeutic options are very scarce and the most sensible approach to tackle this problem is the prevention of contagion.

Since adherence of microorganisms to surfaces leads to the propagation of diseases by simple contact, much effort has been devoted recently to the development of materials with antimicrobial activity.[6] One advanced strategy to deal with the problem of microbial infections is the so-called antimicrobial photodynamic inactivation (aPDI). This preventive / therapeutic approach, related conceptually to the photodynamic therapy (PDT) of cancer,[7] relies on the absorption of light by a photosensitizing molecule which, in the presence of oxygen, is able to generate reactive oxygen species (ROS) capable of killing (or avoiding the growth of) bacteria, virus, fungi, protozoa, and a varied number of other infective agents.[8–11] One of the foreseen applications of aPDI is the prevention of the spreading of microorganism causing diseases by using materials with self-sterilizing surfaces activated by the light used for room illumination.[12,13] The list of elements in a healthcare facility that bacteria can colonize is almost unlimited, including catheters, stethoscopes, armpit thermometers, computer screens, cell phone cases, door handles, wall paints, fabrics, etc. The field of aPDI using immobilized photosensitizers has been reviewed by several groups, [14–17]. Most of the described photosensitizers and many of the polymeric materials use to support them are difficult to synthesize on a large scale, making their use in an extended surface a practical challenge. Hence, from a practical point of view, both photosensitizer and support must be readily accessible and they should be combined in a manner involving simple operational procedures. Here we would like to report two photoactive materials combining the well-known photosentitizer Rose Bengal (**RB**) with two cationic exchange resins differing in their

nature, a macroporous (Amberlite® IRA-900) and a gel-type (Amberlite® IRA-400) cationic polystyrene. The photoactive polymers here presented display outstanding aPDI activity against *P. aeruginosa* when irradiated with visible light, leading to eradication of the population of this microorganism, starting from a concentration of 10^8 colony forming units (CFU) / mL. Many materials have been reported to date within the field of aPDI, but the one here described stands out for its very favorable cost-benefit ratio against one of the top threats identified by the WHO.

2. Materials and methods

2.1. Synthesis of the supported photosensitizers

The preparation of the RB loaded polymers was performed by mixing 50 mL of Rose Bengal sodium salt (**RB**, Sigma-Aldrich) solution in absolute EtOH (30 μM) with 1 g of Amberlite® IRA-900 or Amberlite® IRA-400 (both from Sigma-Aldrich, chloride form; ion exchange resins were previously washed with ethanol and vacuum dried overnight). The suspension was stirred smoothly at room temperature. Loading was followed by UV-Vis (JASCO V-630 UV-vis spectrophotometer), monitoring the decrease of the absorbance at 560 nm (quantitative **RB** loading after 70 min of stirring). The beads were filtered off on a sintered glass filter and washed with EtOH. Finally, the polymers were dried under vacuum at 55 ºC overnight. Characterization of the supported photosensitizers was performed by fluorescence spectroscopy, porosimetry, and scanning electron microscopy (see below).

2.2. Fluorescence Spectroscopy.

The steady-state fluorescence of the samples was recorded with a Varian Cary-Eclipse spectrofluorometer, using quartz cell cuvettes. The polymeric samples were measured in the solid state whereas spectra of **RB** was recorded in solution. In the case of the polymers, five

measurements were carried out for each sample in different areas of the solid and the results were averaged. Excitation wavelength was set at 555 nm. To record the excitation spectra, the emission wavelength was set at 575 nm (**RB** in EtOH) or 600 nm (**RB@P$_{mp}$** and **RB@P$_{gel}$**).

2.3. Porosimetry.

Measurements were carried out on a Micromeritics ASAP 2020 gas porosimeter equipped with a SmartVac degasification system. 1 g of **RB@P$_{mp}$** and **RB@P$_{gel}$** were washed with ethanol and dried for 24 h in a vacuum oven at 60 ºC before performing the analysis.

2.4 Scanning Electron Microscopy.

Images were acquired using a JEOL 7001F scanning electron microscope equipped with a digital camera. The samples were placed on top of a tin plate and sputtered with Pt in a Bal-tec SCD500 sputter coater.

2.5. Benchmark model reaction for measuring $^1O_2$ production.

Photooxygenation reactions were conducted inside open flasks containing aerated solutions of the $^1O_2$ trap (50 mL, DMA $1x10^{-4}$ M) in the corresponding solvent (acetonitrile, absolute ethanol or EtOH: H_2O, 1:1, v:v) and 500 mg of **RB@P$_{mp}$** or **RB@P$_{gel}$**. The mixtures were irradiated (20 minutes were enough to obtain reliable kinetic traces), with continuous stirring, using two light-emitting diode (LED) lamps (11 W each, Lexman, ca. 400–700 nm; 15.6 mW/cm^2) placed 3 cm away from the reaction flask. The photooxygenation reaction was monitored by means of UV-Vis absorption, following the decrease of the absorbance at 376 nm in a JASCO V-630 UV-Vis spectrophotometer. The kinetic traces were fitted to a pseudo-first order model ($\ln C/C_0 = -k_{obs} \cdot t$, where C is the concentration of DMA at a certain time t and C_0 is the initial concentration

of DMA; for low concentrations of substrate, the concentration ratio C/C_0 is considered to be equivalent to the absorbance ratio A/A_0).

2.6. Photooxygenation cycles.

Irradiations were performed as indicated above (20 minutes to obtain the rate constant),. After complete reaction of the DMA substrate (1h irradiation), the polymer was easily separated by filtration and re-suspended in 50 mL of $1x10^{-4}$ M DMA freshly prepared solution in the corresponding solvent, and irradiated again, up to seven cycles.

2.7. Antibacterial photodynamic studies

P. aeruginosa ATCC 27853, was acquired from the American Type Culture Collection (ATCC, Rockville, MD, USA).

Microorganisms seeded on Columbia Blood Agar (BA) (Oxoid®; Madrid, Spain) were cultured aerobically overnight at 35 °C. The inoculum was prepared in distilled water (Gibco®, Thermofisher, Spain) and adjusted to 0.50 ± 0.03 on the McFarland scale (microbial suspensions containing $>10^8$ bacteria/mL).

Ten groups of samples were prepared: five for the irradiation and five as controls in the darkness. 5 mL of the microbial suspensions were dropped into different RODAC plates (diameter: 5 cm) and then (I) 200 mg of $\mathbf{P_{mp}}$ loaded with **RB** ($\mathbf{RB@P_{mp}}$), or (II) the same amount of control $\mathbf{P_{mp}}$ matrix ($\mathbf{P_{mp}}$ resin without **RB**), or (III) 200 mg of $\mathbf{P_{gel}}$ loaded with **RB** ($\mathbf{RB@P_{gel}}$), or (IV) the same amount of control $\mathbf{P_{gel}}$ matrix ($\mathbf{P_{gel}}$ resin without **RB**), or (V) no resin were added. Final loading of **RB** was 1.5 mg of **RB** / g of resin, i.e., a concentration of 60 µg / mL (200 mg of $\mathbf{RB@P_{mp}}$ or $\mathbf{RB@P_{gel}}$ in 5 mL of suspension). The ten groups were shaken during the time of the photodynamic treatment.

Irradiation was performed using a LED lamp (Showtec LED Par 64 Short 18 x RGB 3-in-1 LED, Highlite International B.V. Spain) emitting at 515 ± 10 nm with a fluence up to 200 J/cm^2 (AVASPEC-1024 Fiber Optic Spectrometer) at a distance of 17 cm (irradiance 5.8 mW/cm^2).

Aliquots of the microbial suspensions from the RODAC plates were taken, the appropriate dilutions were made and they were seeded in BA every time equivalent to a 20 J/cm^2 light dose up to a maximum of 200 J/cm^2 (this maximum dose corresponds to 9.6 h of illumination). The aliquots had a volume of 10 μL. The dilutions or the direct seeding in the plates for counting were carried out according to previous experiments in order to count in the range {>0, <200} CFU/plate. Higher volumes of aliquots were taken in cases where, according to the previous experiments, the CFU number in the plate from the aliquot of 10 μL planted undiluted was 0 (i.e. bacterial growth is expected to be <100 CFU/mL. For samples where the logarithmic reduction reaches or exceeds 6 $\log_{10}$ (<100 CFU/mL), the volumes removed were 100 μl (from these points of reduction). The maximum volume taken was 1 mL (20%) in the points where the logarithmic reduction reaches or exceeds 7 $\log_{10}$ (<10 CFU/mL). After completing the aPDI protocol, samples and controls were incubated overnight at 35 °C. The antibacterial effect was determined by counting the number of CFU/mL on BA using a Flash and Go automatic colony counter (IUL, S.A, Spain). All experiments were carried out at least three times.

3. Results and discussion

Amberlite® IRA-900 is a popular commercial ion exchange resin used in catalysis, chromatography and environmental remediation.[18] It consists basically of macroporous crosslinked polystyrene containing trimethylammonium groups (with chloride as counterion). On the other hand, Amberlite® IRA-400 presents a lower degree of cross-linking which does not allow

a permanent porosity, but can be swollen in appropriate organic solvents, leading to gel-like materials. In the past we have employed synthetic macroporous resins with **RB** attached covalently and studied their photochemical and photobiological properties, including their PDT activity against melanoma cells.[19] In order to facilitate the synthetic methodology, recently we turned our attention to commercial Amberlite® resins IRA 900 and 400 (called from now on $\mathbf{P_{mp}}$ and $\mathbf{P_{gel}}$, respectively). The possibility of carrying out a simple anion exchange (replacing chloride anion by any anionic photosensitizer) makes them very appropriate for the production of large amounts (multigram scale) of photoactive materials in a very straightforward manner. In the field of photocatalysis this is a common method to produce, for instance, photocatalytic materials for oxygenations.[20] In previous reports we used this ion exchange strategy to explore the possibilities of molybdenum-based photosensitizers bound to cationic polymers.[21,22] We found that both supports, $\mathbf{P_{mp}}$ and $\mathbf{P_{gel}}$, are appropriate for the development of photobactericidal materials, against planktonic cultures of *S. aureus* and *P. aeruginosa*, with a better performance of the $\mathbf{P_{mp}}$ resin over the $\mathbf{P_{gel}}$ one. In order to expand the range of useful photosensitizers employing this strategy, we decided to use **RB**, providing its dianionic nature, and considering that it is one of the most studied photo-antimicrobials so far, that it is safe for human use and also that its cost is very low, which could be a practical advantage for future application in real medical contexts.

The above mentioned exchange process is depicted in Figure 1 for the case of **RB**. From the experimental point of view, the procedure is very straightforward: the addition of 1 g of polymer to a 50 mL solution of **RB** (30 μM) in ethanol leads to complete discoloration of the stirred solution after 70 min. The exchange kinetics are very similar for both resins and leads to a red solid that is isolated by filtration. In Figure 1, pictures of resins before and after loading with

RB are shown. It must be noted that both resins were loaded with 1.5 mg of **RB** per gram of polymer, but this loading is not optimized, and could be improved in the future.

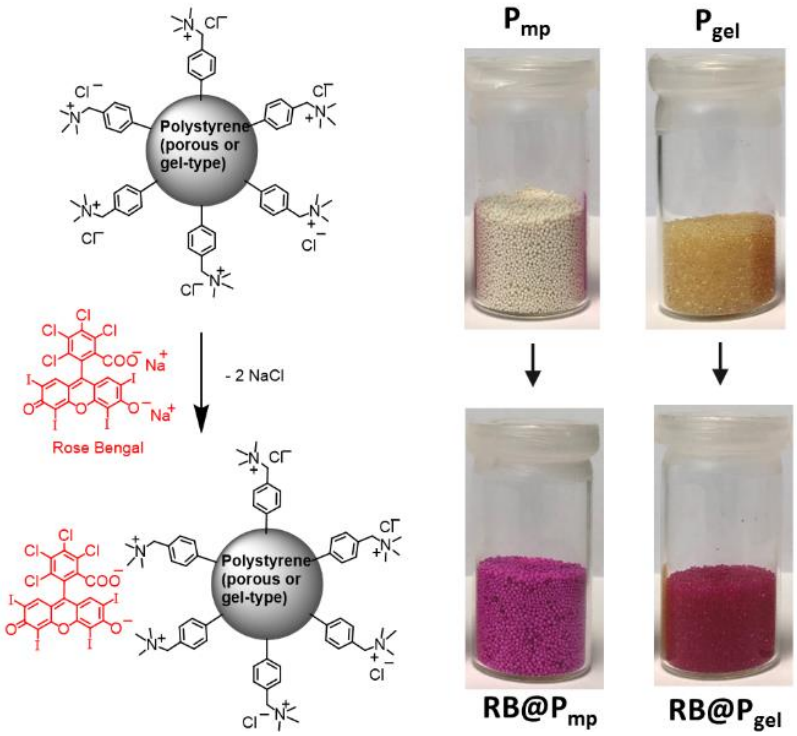

Figure 1. Anionic exchange process to obtain the supported photosensitizers **RB@P$_{mp}$** and **RB@P$_{gel}$** from **RB** and the cationic resins **P$_{mp}$** and **P$_{gel}$**, respectively.

The samples were examined by means of Diffuse Reflectance spectroscopy but very scattered signals were obtained (not shown). Instead, Fluorescence Emission spectroscopy resulted much more informative. The emission and excitation spectra of solid samples of the polymers (Figure 2) revealed the presence of **RB** in a hydrophobic environment (the polymeric matrix), in accordance to the literature (excitation and emission bands are shifted towards longer wavelengths as compared to the spectra of free **RB** in ethanol solution).[23,24] The different visual aspect of the polymers (Figure 1) could be attributable to the slight differences found in the emissive properties of the materials.

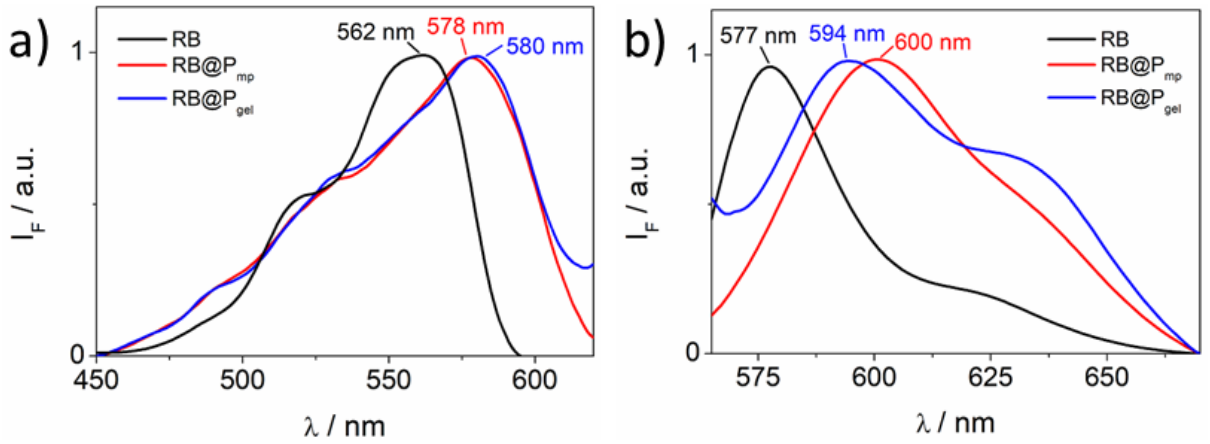

Figure 2. (a) Excitation spectra of **RB** in EtOH, **RB@P$_{mp}$** and **RB@P$_{gel}$** (both polymers in the solid state); Emission monitored at 600 nm. (b) Emission spectra of **RB** in EtOH, **RB@P$_{mp}$** and **RB@P$_{gel}$** (both polymers in the solid state); Excitation set at 550 nm.

The structural properties of the materials were checked by nitrogen porosimetry (see Figure S1 in Supplementary Material). This technique showed much higher values of specific surface for **RB@P$_{mp}$** (21.96 $m^2\ g^{-1}$) than for **RB@P$_{gel}$** (0.0065 $m^2\ g^{-1}$), as expected. The different nanostructure of the matrices were better visualized using Scanning Electron Microscopy (SEM, Figure S2 in Supplementary Material). Images of both materials magnified 50 times show spherical beads very similar in appearance, but a closer look at the nanoscale level (50,000 times magnification), affords a much different view: **RB@P$_{mp}$** is comprised of a structured surface with large and small pores whereas **RB@P$_{gel}$** has a more dense appearance.

The ability of **RB** to induce bacterial killing is based on the production of singlet oxygen ($^1O_2$) upon irradiation with visible light.[25] In order to demonstrate the production of $^1O_2$ species and to compare both photoactive polymers, a benchmark reaction like the oxygenation of 9,10-dimethylanthracene (DMA) was used (Figure 3). In this reaction, the absorption of the DMA probe at 350-400 nm is progressively bleached upon reaction with $^1O_2$ to form the corresponding non-absorbing endoperoxide (DMA·O_2). Monitoring the absorption of DMA *vs* the irradiation time

allows the determination of the pseudo-first order kinetic constant (*k*), which can be used as a relative guide to estimate the photoactivity of the material (Figure 3b).[26] In our case, the two polymers under study were tested using DMA as $^1O_2$ trap, in different solvents. As it can be seen in Figure 3c, the macroporous resin performs the oxygenation reaction in a more effective way than the gel-type material, especially in acetonitrile (ACN). The effect of the solvent on the kinetics of the reaction is attributable to the longer lifetime of $^1O_2$ in acetonitrile as compared to ethanol and water, as reported in the literature.[27] Control irradiations using polymers without photosensitizer afforded minimal values of *k* (2 – 8 x 10^{-3} min^{-1}) as a result of self-photosensitization (DMA absorption tail around 400 nm could be the cause of a slight excitation of the probe leading to residual $^1O_2$ production)

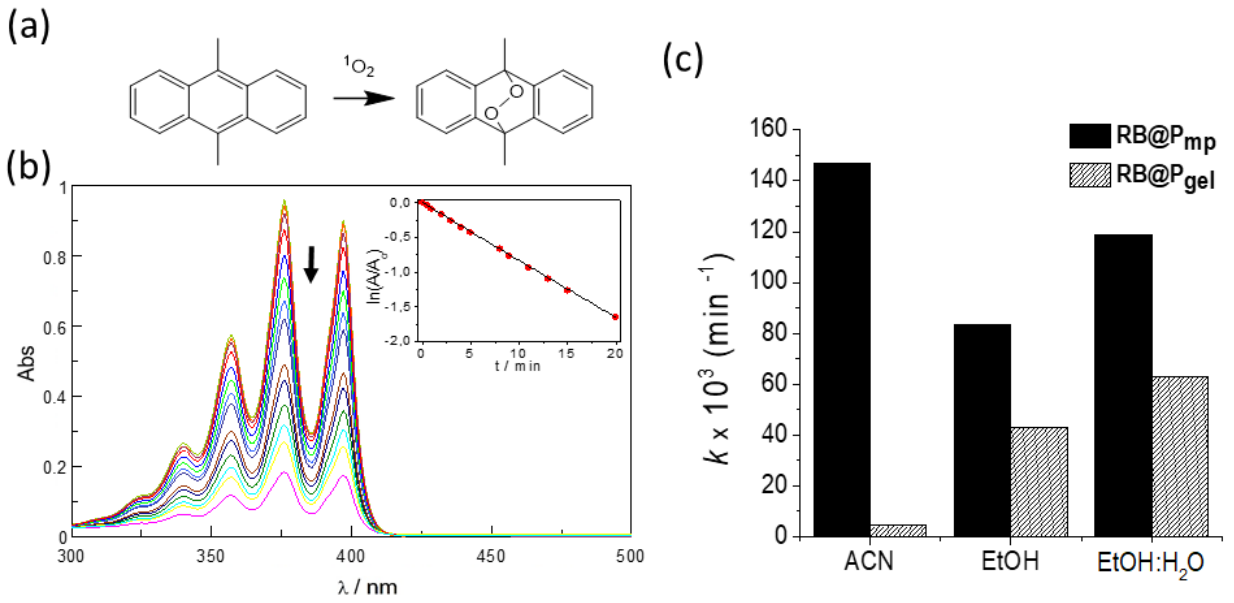

Figure 3. (a) Reaction between 9,10-dimethylanthracene (DMA) and singlet oxygen ($^1O_2$) photosynthesized by **RB@P$_{gel}$** and **RB@P$_{mp}$**. (b) Representative example: UV-Vis spectral variations upon photooxygenation of DMA by $^1O_2$ in ethanol by **RB@P$_{mp}$**; inset: pseudo-first order kinetics fitting (lnA/A_0 vs time). (c) Pseudo-first order kinetic constants corresponding to reactions sensitized with **RB@P$_{gel}$** and **RB@P$_{mp}$** in acetonitrile (ACN), EtOH and EtOH : H_2O (1:1, v:v).

In order to test the resistance of the materials to photobleaching, cycles of irradiations, using the reactivity of DMA as a test, were conducted. As it can be seen in Figure 4, both **RB@P$_{mp}$** and **RB@P$_{gel}$** are effective for seven cycles of oxygenation reactions, with low loss of activity.

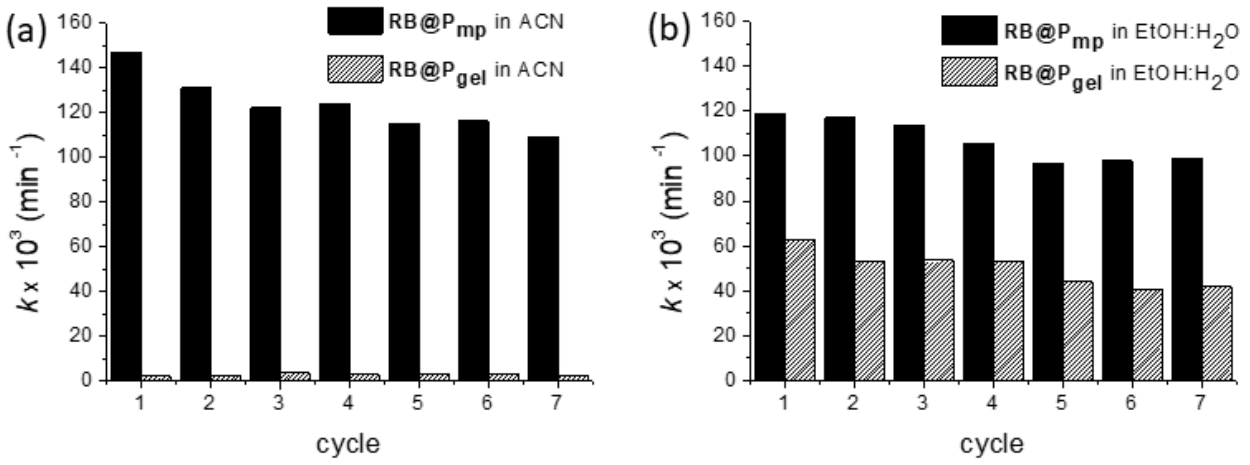

Figure 4. Photooxygenation cycles of DMA with the same sample of **RB@P$_{mp}$** and **RB@P$_{gel}$** in (a) acetonitrile (ACN) and (b) EtOH : H_2O (1:1, v:v).

The polymeric matrices containing **RB** were irradiated in the presence of cultures (10^8 CFU / mL initial concentration) of *Pseudomonas aeruginosa* (Figure 5 and Figure S3 in Supplementary Material). A high killing efficiency was observed with both materials. This result is very remarkable since it is well known that this Gram-negative species is particularly resistant to photodynamic treatments, due to their double protective membrane structure. This is even more striking when considering that it is a well-stablished fact that anionic photosensitizers like **RB** are not particularly effective against Gram-negative species.[28] As a matter of fact, it has been reported that **RB** alone is very inefficient against *P. aeruginosa*.[29] Survival data at a fluence of 120 J/cm^2 can be seen in Figure 5. The effect of **RB@P$_{mp}$** is very remarkable since no CFU can be detected after the irradiation period (8 $\log_{10}$ CFU/mL reduction). In the case of **RB@P$_{gel}$** the result is also very notable, with an estimated 7 $\log_{10}$ CFU/mL reduction (a longer irradiation dose

of 140 J/cm^2 led also to the eradication of this bacteria, see Figure S3 in Supplementary Material). But the action of $^1O_2$ is not the only factor to be considered in order to explain these results since a remarkable reduction of viability is also observed with resins **P_{mp}** and **P_{gel}** (with no **RB** encapsulated inside, third and fourth bars in Figure 5) which induce a reduction of CFU/mL of approximately 3 $\log_{10}$ units for **P_{gel}** and 4 $\log_{10}$ units for **P_{mp}** Hence, to understand the total killing of *P. aeruginosa* upon irradiation the role of the matrix must be taken into account, in addition to the bactericidal effect of the photogenerated $^1O_2$. The antimicrobial effect of ammonium, phosphonium, sulfonium groups and other cationic functionalities present on polymeric and non-polymeric materials has been widely reported in the literature.[30–33] The morphology and other features of the surfaces are also factors that must be taken into account since bacteria could stick to the surface by electrostatic forces, or the lipopolysaccharide (LPS) wall of Gram negative bacteria could be disrupted, as it has been reported in the literature.[34]

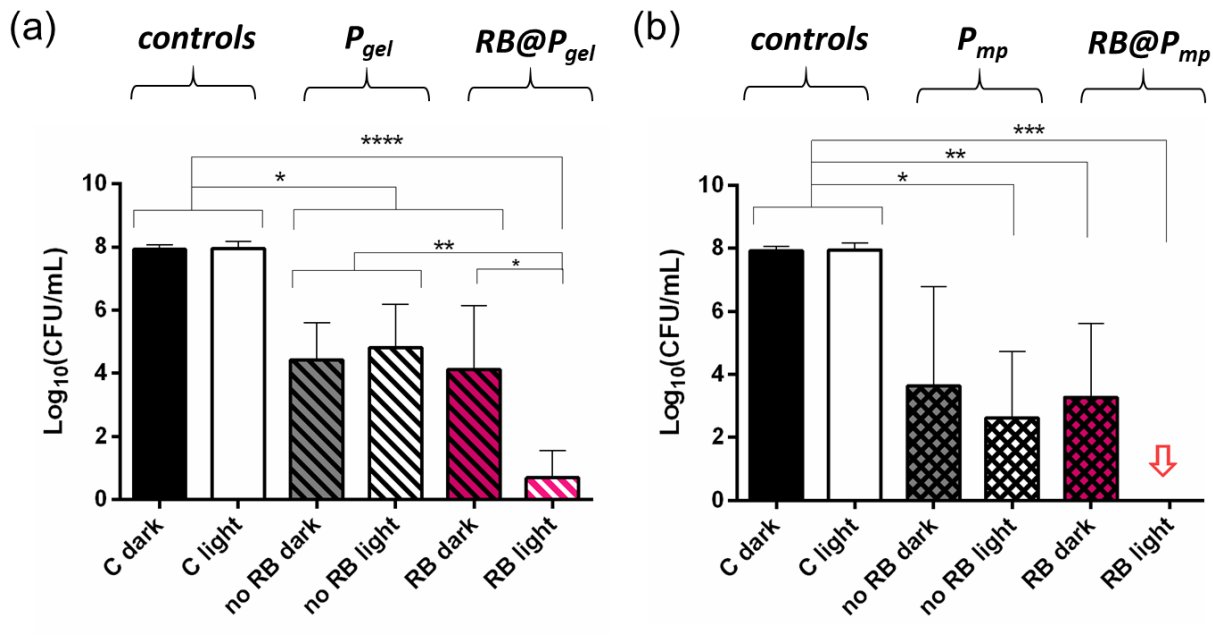

Figure 5. Photodynamic inactivation assays at a fluence of 120 J/cm^2. Inactivation of *P. aeruginosa* with **RB@P$_{gel}$** (left) and **RB@P$_{mp}$** (right). In this graph C is control, only microbial suspension and **RB** means polymer with Rose Bengal. The red arrow indicates 99.999999% reduction of bacterial population. The error bars represent the standard deviation calculated for three measurements. One-way ANOVA statistical analysis: * $p < 0.05$; ** $p < 0.01$; *** $p < 0.001$; **** $p < 0.0001$.

Importantly, the results here reported are consistent with the previously reported effect of similar materials developed in our laboratories. As indicated previously, **P$_{mp}$** and **P$_{gel}$** loaded with a photoactive hexanuclear molybdenum cluster (**Mo$_6$**) were also efficient against *P. aeruginosa* although with a more limited effect. Hence, at 120 J/cm^2, **Mo$_6$@P$_{mp}$** was able to reduce the population of this bacteria ca. 3 $\log_{10}$ CFU/mL whereas **Mo$_6$@P$_{gel}$** did it only by ca. 1 $\log_{10}$ CFU/mL.[22]

Probably, a combination of factors would explain the performance of **RB@P$_{mp}$** towards *P. aeruginosa* here reported: the appropriate distribution of ammonium groups on the polymer, the right nanostructure of the surface, the ability of the surface to bind (and sequester) the bacteria, the

high yield of $^1O_2$ generated by **RB** at the employed concentration and maybe the manufacturing process (and even commercial batch) of the resin. Since those factors are not optimized yet, it is expected that a deeper knowledge of these materials will lead to an improved balance between them and hence it will allow obtaining polymeric materials with even a better performance. Besides, it must be noted that ion-exchange resins must be operated within a certain temperature range in order to maintain their properties [35], so this factor must also be taken into account.

In order to appreciate the value of the reported 8 $\log_{10}$ CFU /mL reduction, a comparison to recently described photosensitizing systems active against *P. aeruginosa* is presented in Table 1. We are aware that different experimental setups make the comparison very difficult (concentrations, bacterial types, excitation wavelengths, light fluences, etc). The presented data do not constitute a systematic revision of the current literature, but an overview of recent results in order to illustrate the value of the cost-effective proposal here presented. We have included only studies in planktonic suspension, not in biofilms,[36] which use a different methodological approach.

Table 1. Reduction of *P. aeruginosa* population caused by soluble and supported photosensitizers reported in literature.

Photosensitizer	**Support**	**Initial load[a]**	**Load reduction[b]**	**Ref.**
Cationic phthalocyanines	-	8-9	-(4-6)	[28]
Cationic fullerenes	-	8	-(2-5)	[37]
Peptide modified porphyrin	-	7	-2	[38]
Cationic porphyrins	-	8	-7	[39]
Cationic porphycenes	-	8	-6	[40]
Photofrin	-	8	0	[41]
Photofrin + 100 mM KI	-	8	-7	[41]
Rose Bengal	-	8	0	[29]
Rose Bengal + 25 mM KI		8	-7	[29]
Gallium phthalocyanine + HasA protein	-	8	-4	[42]
Toluidine blue O	Cellulose acetate	6	-4	[12]
Toluidine blue O	Chitosan	8	-8	[43]
Erythrosine	Chitosan nanoparticles	8	-3.5	[44]
Cationic porphyrin	Cellulose nanocrystals	8	-3	[45]
Cationic porphyrin	Cellulose paper	8	-3.5	[46]
Bodipy	Cellulose paper	8	-2.5	[46]
Azure A	Porous wool keratin	8	-6	[47]
Porphyrin TTFAP	Porous wool keratin	8	0	[47]
Porphyrine TPPS	Polycarboxylic acid	8	0	[48]
Methylene blue	Silica porous NPs	8	-8	[49]
Rose Bengal	Wool/acrylic fabric	8	-1.9	[50]
$[Mo_6I_8I_6]^{2-}$	Fluoropolymer (F-32L)	3	-2	[51]
$[Mo_6I_8Ac_6]^{2-}$	P_{mp} (IRA900)	8	-3	[22]
$[Mo_6I_8Ac_6]^{2-}$	P_{mp} (IRA400)	8	-1	[22]
Rose Bengal	P_{mp} (IRA900)	8	-8	This work
Rose Bengal	P_{gel} (IRA400)	8	-7	This work

(a) Initial load: $\log_{10}$ CFU/mL; (b) Load reduction: $\Delta\log_{10}$ CFU/mL

As can be seen in Table 1, the reductions of the bacterial populations of *P. aeruginosa* caused by both soluble and supported photosensitizers range typically from 1 to 7 $\log_{10}$ CFU / mL. Values of 8 are obtained for methylene blue encapsulated in porous silica nanoparticles[49] and for chitosan used as carrier of Toluidine blue O.[43] However, according to the authors,[43,49]

the action of these supports in the dark against *P. aeruginosa* is negligible. By contrast, $\mathbf{P_{mp}}$ and $\mathbf{P_{gel}}$ polymers already display a dark antibacterial activity (4-5 $\log_{10}$) which would make those polymers still bactericidal against *P. aeruginosa* even when the material is not illuminated.

4. Conclusions

In summary, the aPDI capacity of two new materials, **RB@$\mathbf{P_{mp}}$** and **RB@$\mathbf{P_{gel}}$**, made from easily accessible sources, against *P. aeruginosa* bacteria, has been explored. The excellent results obtained make the materials here reported a good tool for the photo-inactivation of one of the most important threats identified by the WHO. We would like to emphasize on the fact that despite anionic photosensitizers have been relegated in favor of cationic ones for the inactivation of Gram-negative bacteria, if such anionic molecules are combined with simple cationic materials like exchange resins Amberlite® IRA-900 or IRA-400, they could be actually highly effective against resistant microorganism. We expect that the proper combinations of support and photosensitizer, tailored for each pathogen, will be discovered in the coming years, which will help to stop the spreading of pathogenic microorganisms.

Declaration of competing interest

The authors declare no competing financial interest.

Acknowledgements

Ministerio de Ciencia, Innovación y Universidades of Spain (grant RTI2018-101675-B-I00) is acknowledged. F. G. Universitat Jaume I (grant UJI-B2018-30) for the financial support. This study was also supported by the Aragón Government: Infectious Diseases of Difficult Diagnosis and Treatment research group (GIIS-023). I. M. R. thanks the Generalitat Valenciana for a

Santiago Grisolía fellowship (GRISOLIAP/2018/071). R. G. thanks Universitat Jaume I for a postdoctoral fellowship (POSDOC-B/2018/09). C. F.-L. thanks the Ministerio de Economía y Competitividad of Spain for a FPI fellowship (BES-2013-063296). Technical support from SCIC/UJI (J. Gómez, M. C. Peiró) is also acknowledged.

Appendix A. Supplementary data

Supplementary information is available and free of charge: porosimetry curves of the polymers; SEM pictures of the polymers; survival curves of *P. aeruginosa*.

References

[1] K. Bush, P. Courvalin, G. Dantas, J. Davies, B. Eisenstein, P. Huovinen, G.A. Jacoby, R. Kishony, B.N. Kreiswirth, E. Kutter, S.A. Lerner, S. Levy, K. Lewis, O. Lomovskaya, J.H. Miller, S. Mobashery, L.J.V. Piddock, S. Projan, C.M. Thomas, A. Tomasz, P.M. Tulkens, T.R. Walsh, J.D. Watson, J. Witkowski, W. Witte, G. Wright, P. Yeh, H.I. Zgurskaya, Tackling antibiotic resistance, Nat. Rev. Microbiol. 9 (2011) 894–896. https://doi.org/10.1038/nrmicro2693.

[2] L.B. Rice, Federal Funding for the Study of Antimicrobial Resistance in Nosocomial Pathogens: No ESKAPE, J. Infect. Dis. 197 (2008) 1079–1081. https://doi.org/10.1086/533452.

[3] S.R. Shrivastava, P.S. Shrivastava, J. Ramasamy, World health organization releases global priority list of antibiotic-resistant bacteria to guide research, discovery, and development of new antibiotics, JMS - J. Med. Soc. 32 (2018) 76–77. https://doi.org/10.4103/jms.jms_25_17.

[4] G. Otis, S. Bhattacharya, O. Malka, S. Kolusheva, P. Bolel, A. Porgador, R. Jelinek,

Selective Labeling and Growth Inhibition of Pseudomonas aeruginosa by Aminoguanidine Carbon Dots, ACS Infect. Dis. 5 (2019) 292–302. https://doi.org/10.1021/acsinfecdis.8b00270.

[5] E.S. Cândido, M.H. Cardoso, L.Y. Chan, M.D.T. Torres, K.G.N. Oshiro, W.F. Porto, S.M. Ribeiro, E.F. Haney, R.E.W. Hancock, T.K. Lu, C. de la Fuente-Nunez, D.J. Craik, O.L. Franco, Short Cationic Peptide Derived from Archaea with Dual Antibacterial Properties and Anti-Infective Potential, ACS Infect. Dis. 5 (2019) 1081–1086. https://doi.org/10.1021/acsinfecdis.9b00073.

[6] X. Ding, S. Duan, X. Ding, R. Liu, F.J. Xu, Versatile Antibacterial Materials: An Emerging Arsenal for Combatting Bacterial Pathogens, Adv. Funct. Mater. 28 (2018) 1–19. https://doi.org/10.1002/adfm.201802140.

[7] D.W. Felsher, Cancer revoked: Oncogenes as therapeutic targets, Nat. Rev. Cancer. 3 (2003) 375–380. https://doi.org/10.1038/nrc1070.

[8] M. Wainwright, T. Maisch, S. Nonell, K. Plaetzer, A. Almeida, G.P. Tegos, M.R. Hamblin, Photoantimicrobials—are we afraid of the light?, Lancet Infect. Dis. 17 (2017) e49–e55. https://doi.org/10.1016/S1473-3099(16)30268-7.

[9] F. Cieplik, D. Deng, W. Crielaard, W. Buchalla, E. Hellwig, A. Al-Ahmad, T. Maisch, Antimicrobial photodynamic therapy–what we know and what we don't, Crit. Rev. Microbiol. 44 (2018) 571–589. https://doi.org/10.1080/1040841X.2018.1467876.

[10] Q. Jia, Q. Song, P. Li, W. Huang, Rejuvenated Photodynamic Therapy for Bacterial Infections, Adv. Healthc. Mater. 8 (2019) 1–19. https://doi.org/10.1002/adhm.201900608.

[11] M.R. Hamblin, H. Abrahamse, Can light-based approaches overcome antimicrobial resistance?, Drug Dev. Res. 80 (2019) 48–67. https://doi.org/10.1002/ddr.21453.

[12] M. Wilson, Light-Activated Antimicrobial Coating for the Continuous Disinfection of Surfaces, Infect. Control Hosp. Epidemiol. 24 (2003) 782–784. https://doi.org/10.1086/502136.

[13] S. Noimark, C.W. Dunnill, I.P. Parkin, Shining light on materials - A self-sterilising revolution, Adv. Drug Deliv. Rev. 65 (2013) 570–580. https://doi.org/10.1016/j.addr.2012.07.003.

[14] C. Spagnul, L.C. Turner, R.W. Boyle, Immobilized photosensitizers for antimicrobial applications, J. Photochem. Photobiol. B Biol. 150 (2015) 11–30. https://doi.org/10.1016/j.jphotobiol.2015.04.021.

[15] L. Jiang, C.R.R. Gan, J. Gao, X.J. Loh, A Perspective on the Trends and Challenges Facing Porphyrin-Based Anti-Microbial Materials, Small. 12 (2016) 3609–3644. https://doi.org/10.1002/smll.201600327.

[16] M.Q. Mesquita, C.J. Dias, M.G.P.M.S. Neves, A. Almeida, M.A.F. Faustino, Revisiting current photoactive materials for antimicrobial photodynamic therapy, Molecules. 23 (2018) 2424. https://doi.org/10.3390/molecules23102424.

[17] N. Maldonado-Carmona, T.S. Ouk, M.J.F. Calvete, M.M. Pereira, N. Villandier, S. Leroy-Lhez, Conjugating biomaterials with photosensitizers: Advances and perspectives for photodynamic antimicrobial chemotherapy, Photochem. Photobiol. Sci. 19 (2020) 445–461. https://doi.org/10.1039/c9pp00398c.

[18] P. Barbara, F. Liguori, Ion exchange resins: Catalyst recovery and recycle, Chem. Rev. 109 (2009) 515–529. https://doi.org/10.1021/cr800404j.

[19] M.I. Burguete, F. Galindo, R. Gavara, S.V. Luis, M. Moreno, P. Thomas, D.A. Russell, Singlet oxygen generation using a porous monolithic polymer supported photosensitizer:

Potential application to the photodynamic destruction of melanoma cells, Photochem. Photobiol. Sci. 8 (2009). https://doi.org/10.1039/b810921d.

[20] P. Kubát, P. Henke, V. Berzediová, M. Štěpánek, K. Lang, J. Mosinger, Nanoparticles with Embedded Porphyrin Photosensitizers for Photooxidation Reactions and Continuous Oxygen Sensing, ACS Appl. Mater. Interfaces. 9 (2017) 36229–36238. https://doi.org/10.1021/acsami.7b12009.

[21] A. Beltrán, M. Mikhailov, M.N. Sokolov, V. Pérez-Laguna, A. Rezusta, M.J. Revillo, F. Galindo, A photobleaching resistant polymer supported hexanuclear molybdenum iodide cluster for photocatalytic oxygenations and photodynamic inactivation of: Staphylococcus aureus, J. Mater. Chem. B. 4 (2016) 5975–5979. https://doi.org/10.1039/c6tb01966h.

[22] C. Felip-León, C. Arnau Del Valle, V. Pérez-Laguna, M. Isabel Millán-Lou, J.F. Miravet, M. Mikhailov, M.N. Sokolov, A. Rezusta-López, F. Galindo, Superior performance of macroporous over gel type polystyrene as a support for the development of photo-bactericidal materials, J. Mater. Chem. B. 5 (2017) 6058–6064. https://doi.org/10.1039/c7tb01478c.

[23] M.I. Burguete, R. Gavara, F. Galindo, S.V. Luis, New polymer-supported photocatalyst with improved compatibility with polar solvents. Synthetic application using solar light as energy source, Catal. Commun. 11 (2010). https://doi.org/10.1016/j.catcom.2010.05.013.

[24] M.I. Burguete, R. Gavara, F. Galindo, S.V. Luis, Synthetic application of photoactive porous monolithic polymers, Tetrahedron Lett. 51 (2010) 3360–3363. https://doi.org/10.1016/j.tetlet.2010.04.065.

[25] V. Pérez-Laguna, I. García-Luque, S. Ballesta, L. Pérez-Artiaga, V. Lampaya-Pérez, S. Samper, P. Soria-Lozano, A. Rezusta, Y. Gilaberte, Antimicrobial photodynamic activity

of Rose Bengal, alone or in combination with Gentamicin, against planktonic and biofilm Staphylococcus aureus, Photodiagnosis Photodyn. Ther. 21 (2018) 211–216. https://doi.org/10.1016/j.pdpdt.2017.11.012.

[26] R. Bresolí-Obach, J. Nos, M. Mora, M.L. Sagristà, R. Ruiz-González, S. Nonell, Anthracene-based fluorescent nanoprobes for singlet oxygen detection in biological media, Methods. 109 (2016) 64–72. https://doi.org/10.1016/j.ymeth.2016.06.007.

[27] M. Bregnhøj, M. Westberg, F. Jensen, P.R. Ogilby, Solvent-dependent singlet oxygen lifetimes: Temperature effects implicate tunneling and charge-transfer interactions, Phys. Chem. Chem. Phys. 18 (2016) 22946–22961. https://doi.org/10.1039/c6cp01635a.

[28] A. Minnock, D.I. Vernon, J. Schofield, J. Griffiths, J.H. Parish, S.B. Brown, Photoinactivation of bacteria. Use of a cationic water-soluble zinc phthalocyanine to photoinactivate both gram-negative and gram-positive bacteria, J. Photochem. Photobiol. B Biol. 32 (1996) 159–164. https://doi.org/10.1016/1011-1344(95)07148-2.

[29] P. Iodide, P. Antimicrobial, crossm Potassium Iodide Potentiates Antimicrobial, 61 (2017) 1–15.

[30] E.R. Kenawy, S.D. Worley, R. Broughton, The chemistry and applications of antimicrobial polymers: A state-of-the-art review, Biomacromolecules. 8 (2007) 1359–1384. https://doi.org/10.1021/bm061150q.

[31] I. Banerjee, R.C. Pangule, R.S. Kane, Antifouling coatings: Recent developments in the design of surfaces that prevent fouling by proteins, bacteria, and marine organisms, Adv. Mater. 23 (2011) 690–718. https://doi.org/10.1002/adma.201001215.

[32] D.M. Brown, J. Yang, E.W. Strach, M.I. Khalil, D.G. Whitten, Size and Substitution Effect on Antimicrobial Activity of Polythiophene Polyelectrolyte Derivatives Under Photolysis

and Dark Conditions †, (2018) 1116–1123. https://doi.org/10.1111/php.13013.

[33] A. Muñoz-Bonilla, M. Fernández-García, Polymeric materials with antimicrobial activity, Prog. Polym. Sci. 37 (2012) 281–339. https://doi.org/10.1016/j.progpolymsci.2011.08.005.

[34] D.P. Linklater, S. Juodkazis, E.P. Ivanova, Nanofabrication of mechano-bactericidal surfaces, Nanoscale. 9 (2017) 16564–16585. https://doi.org/10.1039/c7nr05881k.

[35] E.W. Baumann, Thermal Decomposition of Amberlite IRA-400, J. Chem. Eng. Data. 5 (1960) 376–382. https://doi.org/10.1021/je60007a040.

[36] A. Shrestha, M.R. Hamblin, A. Kishen, Characterization of a conjugate between rose bengal and chitosan for targeted antibiofilm and tissue stabilization effects as a potential treatment of infected dentin, Antimicrob. Agents Chemother. 56 (2012) 4876–4884. https://doi.org/10.1128/AAC.00810-12.

[37] G.P. Tegos, T.N. Demidova, D. Arcila-Lopez, H. Lee, T. Wharton, H. Gali, M.R. Hamblin, Cationic fullerenes are effective and selective antimicrobial photosensitizers, Chem. Biol. 12 (2005) 1127–1135. https://doi.org/10.1016/j.chembiol.2005.08.014.

[38] R. Dosselli, M. Gobbo, E. Bolognini, S. Campestrini, E. Reddi, Porphyrin-apidaecin conjugate as a new broad spectrum antibacterial agent, ACS Med. Chem. Lett. 1 (2010) 35–38. https://doi.org/10.1021/ml900021y.

[39] S. Banfi, E. Caruso, L. Buccafurni, V. Battini, S. Zazzaron, P. Barbieri, V. Orlandi, Antibacterial activity of tetraaryl-porphyrin photosensitizers: An in vitro study on Gram negative and Gram positive bacteria, J. Photochem. Photobiol. B Biol. 85 (2006) 28–38. https://doi.org/10.1016/j.jphotobiol.2006.04.003.

[40] R. Ruiz-González, M. Agut, E. Reddi, S. Nonell, A comparative study on two cationic porphycenes: Photophysical and antimicrobial photoinactivation evaluation, Int. J. Mol. Sci.

16 (2015) 27072–27086. https://doi.org/10.3390/ijms161125999.

[41] L. Huang, G. Szewczyk, T. Sarna, M.R. Hamblin, Potassium Iodide Potentiates Broad-Spectrum Antimicrobial Photodynamic Inactivation Using Photofrin, ACS Infect. Dis. 3 (2017) 320–328. https://doi.org/10.1021/acsinfecdis.7b00004.

[42] Y. Shisaka, Y. Iwai, S. Yamada, H. Uehara, T. Tosha, H. Sugimoto, Y. Shiro, J.K. Stanfield, K. Ogawa, Y. Watanabe, O. Shoji, Hijacking the Heme Acquisition System of Pseudomonas aeruginosa for the Delivery of Phthalocyanine as an Antimicrobial, ACS Chem. Biol. 14 (2019) 1637–1642. https://doi.org/10.1021/acschembio.9b00373.

[43] T. Tsai, H.F. Chien, T.H. Wang, C.T. Huang, Y.B. Ker, C.T. Chen, Chitosan augments photodynamic inactivation of gram-positive and gram-negative bacteria, Antimicrob. Agents Chemother. 55 (2011) 1883–1890. https://doi.org/10.1128/AAC.00550-10.

[44] C.P. Chen, C.T. Chen, T. Tsai, Chitosan nanoparticles for antimicrobial photodynamic inactivation: Characterization and in vitro investigation, Photochem. Photobiol. 88 (2012) 570–576. https://doi.org/10.1111/j.1751-1097.2012.01101.x.

[45] B.L. Carpenter, E. Feese, H. Sadeghifar, D.S. Argyropoulos, R.A. Ghiladi, Porphyrin-cellulose nanocrystals: A photobactericidal material that exhibits broad spectrum antimicrobial activity, Photochem. Photobiol. 88 (2012) 527–536. https://doi.org/10.1111/j.1751-1097.2012.01117.x.

[46] B.L. Carpenter, F. Scholle, H. Sadeghifar, A.J. Francis, J. Boltersdorf, W.W. Weare, D.S. Argyropoulos, P.A. Maggard, R.A. Ghiladi, Synthesis, Characterization, and Antimicrobial Efficacy of Photomicrobicidal Cellulose Paper, Biomacromolecules. 16 (2015) 2482–2492. https://doi.org/10.1021/acs.biomac.5b00758.

[47] C. Ferroni, G. Sotgiu, A. Sagnella, G. Varchi, A. Guerrini, D. Giuri, E. Polo, V.T. Orlandi,

E. Marras, M. Gariboldi, E. Monti, A. Aluigi, Wool Keratin 3D Scaffolds with Light-Triggered Antimicrobial Activity, Biomacromolecules. 17 (2016) 2882–2890. https://doi.org/10.1021/acs.biomac.6b00697.

[48] M.A. Castriciano, R. Zagami, M.P. Casaletto, B. Martel, M. Trapani, A. Romeo, V. Villari, M.T. Sciortino, L. Grasso, S. Guglielmino, L.M. Scolaro, A. Mazzaglia, Poly(carboxylic acid)-Cyclodextrin/Anionic Porphyrin Finished Fabrics as Photosensitizer Releasers for Antimicrobial Photodynamic Therapy, Biomacromolecules. 18 (2017) 1134–1144. https://doi.org/10.1021/acs.biomac.6b01752.

[49] O. Planas, R. Bresolí-Obach, J. Nos, T. Gallavardin, R. Ruiz-González, M. Agut, S. Nonell, Synthesis, photophysical characterization, and photoinduced antibacterial activity of methylene blue-loaded amino- and mannose-targeted mesoporous silica nanoparticles, Molecules. 20 (2015) 6284–6298. https://doi.org/10.3390/molecules20046284.

[50] W. Chen, J. Chen, L. Li, X. Wang, Q. Wei, R.A. Ghiladi, Q. Wang, Wool/Acrylic Blended Fabrics as Next-Generation Photodynamic Antimicrobial Materials, ACS Appl. Mater. Interfaces. 11 (2019) 29557–29568. https://doi.org/10.1021/acsami.9b09625.

[51] N.A. Vorotnikova, A.Y. Alekseev, Y.A. Vorotnikov, D. V. Evtushok, Y. Molard, M. Amela-Cortes, S. Cordier, A.I. Smolentsev, C.G. Burton, P.M. Kozhin, P. Zhu, P.D. Topham, Y. V. Mironov, M. Bradley, O.A. Efremova, M.A. Shestopalov, Octahedral molybdenum cluster as a photoactive antimicrobial additive to a fluoroplastic, Mater. Sci. Eng. C. 105 (2019) 110150. https://doi.org/10.1016/j.msec.2019.110150.